

# WORKSPACE ANALYSIS OF A FLAME INTRA-ROW WEEDING ROBOT IN VEGETABLE FIELD AND NUMERICAL SIMULATION OF PROPANE COMBUSTION

## 蔬菜株间火焰除草机器人工作空间分析与丙烷燃烧数值模拟

Xu Bing<sup>1)</sup>, Zheng Decong<sup>1)\*</sup>, Wang Jiaxin<sup>2)</sup>, Yang Youzhi<sup>3)</sup>

<sup>1)</sup> College of Agricultural Engineering, Shanxi Agricultural University, Taigu / China

<sup>2)</sup> College of Mechanical and Electronic Engineering, Northwest A&F University, Yangling / China

<sup>3)</sup> Quick Intelligent Equipment Co., Ltd, Changzhou / China

Tel: +86-0354-6288339;\*) E-mail: zhengdecong@126.com

DOI: <https://doi.org/10.35633/inmateh-65-08>

**Keywords:** *intra-row weeding, flame weeding, Delta mechanism, workspace, numerical simulation*

### ABSTRACT

A flame intra-row weeding robot, based on the Delta mechanism, was designed to solve the problems of high labor intensity, low efficiency, easy-to-harm seedling and others. Simultaneously, the applicable robot kinematics model was established. Moreover, the method of exhaustion enabled us to obtain the full-scale robot workspace and analyze its smart workspace. When the nozzle diameter took different values, the numerical simulation on the propane combustion process in the burner was performed by the Fluent component transport model, analyzing the temperature distribution inside and out of the burner. The experimental results showed that the flame intra-row weeding robot was required to work on the condition that the radius of smart cylindrical space is  $\Phi 400 \text{ mm} \times 359.8 \text{ mm}$  — when the length of the driving arm is 300 mm, the length of the driven arm is 800 mm, the radius of the static platform is 150 mm and the radius of the movable platform is 50 mm — the maximum temperature of propane flame reaches 1,830 K and the width of the high temperature zone reaches 27 mm — when the nozzle diameter is 1.6 mm.

### 摘要

针对蔬菜株间除草作业劳动强度大、效率低、易伤苗等问题，设计了一种基于 Delta 机构的株间火焰除草机器人，并建立了机器人运动学模型，利用穷举法得到了机器人全工作空间，并对其灵巧工作空间进行了分析；当喷嘴直径取不同值时，基于 Fluent 组分输运模型分别对燃烧器内丙烷燃烧过程进行了数值模拟，对燃烧器内部及出口温度分布进行了分析。结果表明，当主动臂长度为 300 mm、从动臂长度为 800 mm、静平台半径为 150 mm、动平台半径为 50 mm 时，其灵巧工作空间为  $\Phi 400 \text{ mm} \times 359.8 \text{ mm}$  的圆柱形空间，当喷嘴直径为 1.6 mm 时，丙烷火焰最高温度达 1830 K，燃烧器出口高温区宽度达 27 mm，满足株间火焰除草的要求。

### INTRODUCTION

Vegetables are one of the basic food sources for human being, providing vitamins, dietary fiber and minerals necessary for human health (Deng et al., 2018). China's vegetable production and consumption both rank first in the world, but the mechanization of vegetable production is still in the initial stage (Xiao et al., 2017). Easy-to-spread field weeds compete with crops for water, fertilizer and space, leading to a decline in the vegetable production. Therefore, field weeding is an essential part for vegetable production. Field weeds can be divided into the inter-row weeds and the intra-row weeds (Chen et al., 2015; Liu et al., 2017). The traditional cultivating implement is mainly applicable to the inter-row weeds, or when the distance between weeds and seedlings is relatively short, which requires a high demand in the weeding accuracy and thus improves the difficulty of weeding. The manual or the chemical method is often applied to the common weeding. The former is labor-intensive and low-efficiency, while the later reduces labor intensity but improves the weeding efficiency. Nevertheless, a large amount of herbicides not only cause the eutrophication of water bodies and the environmental pollution, but also lead to the pesticide residues in vegetables (Wu et al., 2019; Wang et al., 2018). Therefore, it is of great significance and urgency to develop the intelligent intra-row weeding device to improve the production efficiency and cut down on the use of pesticide in the context of the aging of the agricultural population, the reduction of labor force and the increasing demand for the quality of vegetable.

---

Bing Xu, As Lec. M.S. Eng.; Decong Zheng, Prof. Ph.D. Eng.; Jiaxin Wang M.S. Stud. Eng.; Youzhi Yang M.S. Eng.

Recently, researchers and scholars from various countries have done a lot of research on the intelligent intra-row weeding for different crops under different production conditions. The relevant studies at this stage mainly focus on the structure design, the recognition algorithm on the difference between weeds and seedlings and other key technologies for the intra-row weeding and the end-effector. *Hu Lian et al.* designed a claw-tooth intra-row weeding device that can kill weeds and get out of the way of seedlings by controlling the trochoid motion of claw-tooth (*Hu et al., 2012*). *Huang Xiaolong et al.* optimized the design on the end-effector and carried out the intra-row weeding robot experiment in vegetable field. The experiments results proved that the weeding rate was 95.4% when the plant spacing was 350 mm (*Huang et al., 2012*). The researchers also conducted the structural designs and had experiments on the intra-row weeding devices for crops, such as rice, corn, soybeans and grapes (*Jiang et al., 2020; Zhou et al., 2018; Han et al., 2020; Reiser et al., 2019*). *Kumar Satya Prakash et al.* presents development of a cost-effective mechatronic prototype for intra-row weeding operation. Preliminary field evaluations showed this system to be effective for intra-row weed (>65%) and plant damage control (<25%) (*Kumar et al., 2020*). For vegetable fields at the seedling stage, it is natural that seedlings are weak and the grass is strong. The existing intra-row weeding devices often kill weeds and get out of the way of seedlings by swinging or rotating weeding knives and weeding teeth. Because the distance between weeds and vegetable seedlings is short, this method is easy to harm the shallow root system of vegetable seedlings.

Some scholars tried physical methods to control weeds, such as electric, fire, microwave, steam and others. *Wang Jinwu et al.* designed a water jet weeding device and carried out a bench test, whose experiment results proved that the weeding rate is 90.62% when the water pressure of the device is 1.5 MPa (*Wang et al., 2021*). A flame weeder was applied to the production of organic corns by Serbian scholar *Rajković Miloš (Rajković et al., 2021)*. Generally, by methods of electric, fire, microwave, steam and others, it can reduce the damage to crop roots but can easily damage crop stems and leaves. Hence, it is urgent to improve the weeding rate and precision but reduce the damage rate of seedlings (*Raja et al., 2020a*).

The Delta mechanism is featured with the fast speed and the high precision. Based on this advantage, this paper designed a flame intra-row weeding robot in vegetable fields. It relied on the Delta mechanism and took the burner as the end-effector and the propane as fuel. Equipped with the self-propelled high-clearance platform and the Delta mechanism, it can meet the high-precision requirements of the intra-row weeding. The analysis on the weeding robot workspace and the numerical simulation on the temperature distribution of propane combustion flame by FLUENT confirmed that the Delta mechanism parameters and the burner nozzle diameter meet the requirements of the intra-row flame weeding.

## **MATERIALS AND METHODS**

### **Flame Weeding Operation Environment and Requirements**

Field investigations and relevant literature (*Trygve et al., 2018; Raja et al., 2020b; Kennedy et al., 2020*) inquiry enable us to know different vegetable cultivation modes, which help us determine the intra-row weeding operation environment in vegetable fields. It requires that the plant spacing is 300~500 mm, the plant height is 220~360 mm, and the row spacing is more than 200 mm. The flame weeding utilizes the fuel to produce high-temperature flames and destroy the weed cells and tissues, causing them to quickly lose water and die. The relevant studies indicate that the cytoderm of weeds will be destroyed when the flame temperature reaches 100 °C (about 375 K), which can control the growth of weeds. However, there has been a certain difference among and between different types of weeds and the same type of weeds at different growth stages (*Knezevic et al., 2014*). In order to make the burner have a better effect on most of weeds, the working temperature in the burner is above 600 K, namely the flame temperature is above 600 K. In addition to the flame temperature, the flame form also has an effect on the weed control to reduce its effectiveness and efficiency. The long and narrow flame can kill heat-sensitive weeds that grow in the vertical direction, while the short and wide flame has a good effect on weeds that creep on the ground and have more growing points to increase its weeding efficiency (*Guan et al., 2019; Fu et al., 2016*). On the whole, the flame width in the high temperature zone should be above 25 mm in designing the burner. In addition, the flame weeding should be performed in the condition of no wind or less wind, in which the wind speed is 0~0.2 m/s.

### **Structure and Principle of Flame Weeding Robot**

The flame intra-row weeding robot is mainly composed of self-propelled high-clearance platform, Delta mechanism, vision system, fuel tank, pressure gauge, hose, burner and so on. The Delta mechanism includes mobile platform, driven arm, driving arm, motor and static platform.

The schematic diagram of the field operation of the flame weeding robot is shown in Figure 1. The Figure shows that  $L_1$  represents the plant spacing and  $L_2$  represents the row spacing.

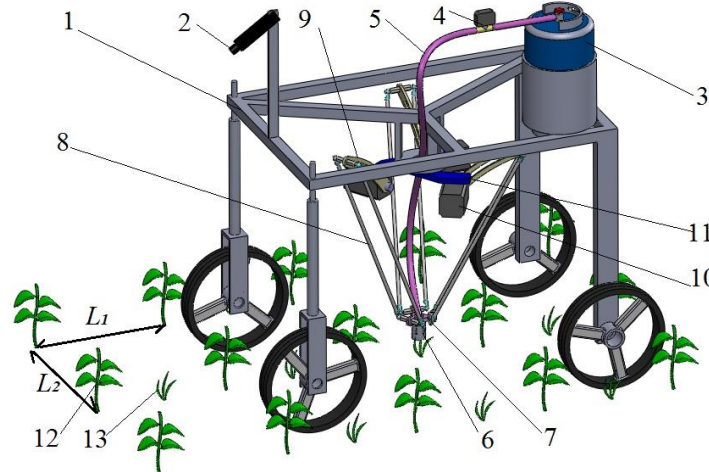


**Fig. 1 - The schematic diagram of the field operation of the flame weeding robot**

1- self-propelled high-clearance platform; 2- vision system; 3- fuel tank; 4- pressure gauge; 5- hose; 6- burner; 7- mobile platform; 8- driven arm; 9- driving arm; 10- motor ; 11- static platform; 12-crop; 13-weeds

The Delta mechanism is fixed on the frame of the self-propelled high-clearance platform by the static platform and the burner is fixed on the mobile platform. The burner is connected with the fuel tank fixed on the frame through the hose. When the weeding robot is working, the walking wheels on both sides of the self-propelled high-clearance platform respectively moved in adjacent crop rows, and the vision system identify crops and weeds to direct the driving arms to place the burner at different positions, killing the weeds and getting out of the way of seedlings.

**Division of Intra-row Weeding Area**

Vegetable seedlings divide the intra-row area into the intra-row weeding area and the protection area, as shown in Figure 2(a). The circular area with a radius of  $l$  represents the protection area and the other circular area with a diameter of  $(L_1-2l)$  represents the intra-row weeding area. The weeding operation of the flame weeding robot is composed of killing weeds and getting out of the way of seedlings. When the weeder is working, the burner, located in the intra-row weeding area, sprays the flame at a position of  $h$  above the ground. As shown in Figure 2(b),  $h$  is 50 mm. On the condition of getting out of the way of seedlings, the burner extinguishes the flame and raises a certain height to cross the protection area and enter into the next intra-row weeding area.

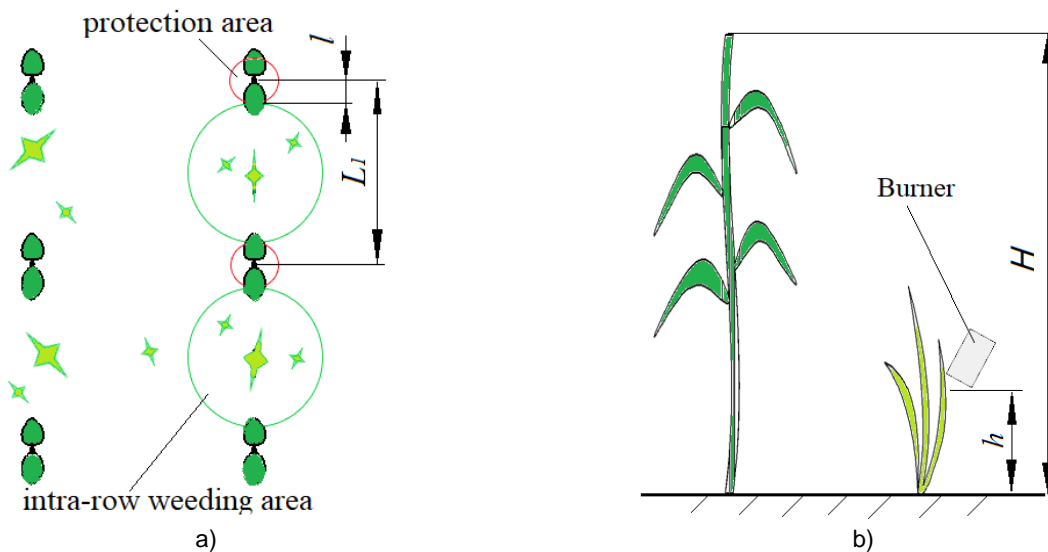


**Fig. 2 - Schematic diagram of division of intra-row weeding area**

Due to the discontinuous intra-row weeding area, it is easy to miss the weeds or harm the seedlings. Hence, the weeding rate and the damage rate of seedlings are two key indicators to measure the effectiveness of intra-row weeding.

The premise of increasing the weeding rate is that the end-effector, namely the burner workspace, can cover the intra-row weeding area to reduce the miss rate, when the weeding robot stays at the intra-row weeding area. To reduce the damage rate of seedlings simultaneously, the burner should be lifted above the height of crops, when the weeding robot leaves the intra-row weeding to pass the protection area.

The Delta mechanism full-scale workspace has a bowl-shaped enveloping space. In practical applications, it is generally applied to a cylindrical and smart workspace (Zhang et al., 2018). When the flame weeding robot is working, the burner is located on the flat surface, that is, the target working platform of the Delta mechanism and the bottom surface of the cylindrical smart workspace, at a position of  $h$  above the ground. The diameter of the bottom surface is represented by  $D$ . To make the burner workspace cover the intra-row weeding area,  $D$  should satisfy the formula (1). The maximum height that the burner can be lifted from the target working platform, namely the height of the cylindrical smart workspace  $H_1$ , should satisfy the formula (2) to help the burner cross the crops and successfully get out of the way of seedlings.

$$D \geq L_1 - 2l \tag{1}$$

$$H_1 \geq H - h \tag{2}$$

To have a wider range, the plant spacing  $L_1$  and the plant height  $H$  for the weeding robots are designed to be the maximum values respectively, namely  $L_1=500$  mm and  $H=360$  mm. Therefore, the bottom diameter  $D$  of the cylindrical smart workspace should be equal to or greater than 400 mm and the  $H_1$  should be greater than 310mm to meet the operational requirements.

**Kinematics Model of Delta Mechanism**

The kinematic equation of the Delta mechanism should be established firstly, to obtain the workspace of the weeding robot. The schematic diagram of the Delta mechanism is shown in Figure 3.  $A_1A_2A_3$  is the static platform and  $C_1C_2C_3$  is the mobile platform.  $A_iB_i$  is the driving arm ( $i=1,2,3$ ) and its length is presented by  $L_b$ . The field angle between the driving arm and the static platform is marked by  $\theta_i$ .  $B_iC_i$  is the driven arm and  $L_a$  represents its length. Taking the static platform center  $O$  as the origin of coordinate, establish the static coordinate system  $O-XYZ$  and make sure that the  $Y$  axis is perpendicular to  $A_1A_2$ . Taking the mobile platform center  $O'$  as the origin of coordinate, establish the static coordinate system.  $OA_i$  represents the radius of the static platform, and its length is  $R$ .  $O' C_i$  represents the radius of the mobile platform and its length is  $r$ . The included angle between  $OA_i$  and the  $X$  axis is defined as  $\eta_i$ .

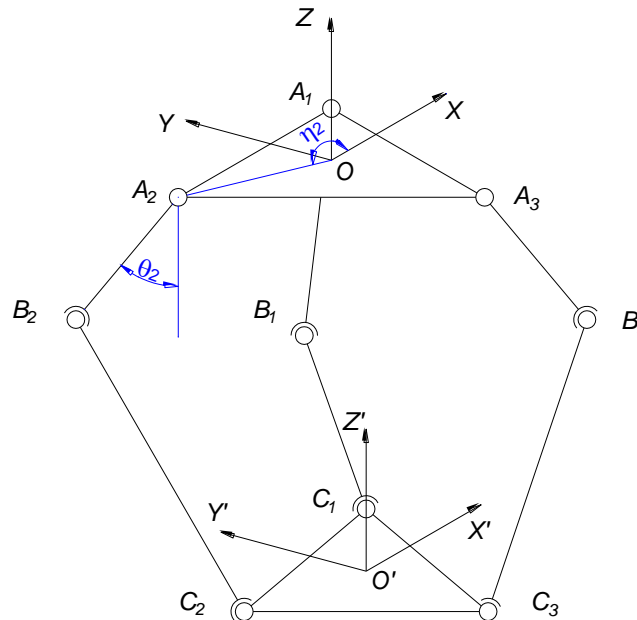


Fig. 3 - Sketch of Delta mechanism

The origin  $O'$  of the mobile coordinate system is represented by  $(x, y, z)$  on the dynamic coordinate system. In accordance with the geometric relationship, all parameters should satisfy the kinematic equation (3) (Zhang et al., 2018):

$$[(R + L_b \sin \theta_i - r) \cos \eta_i - x]^2 + [(R + L_b \sin \theta_i - r) \sin \eta_i - y]^2 + [-L_b \cos \theta_i - z]^2 = L_a^2 \tag{3}$$

Substitute  $\eta_i$  into the equation (3) to obtain the equation set (4).

$$\begin{cases} \left[ \frac{\sqrt{3}}{2} (R + L_b \sin \theta_1 - r) - x \right]^2 + \left[ \frac{1}{2} (R + L_b \sin \theta_1 - r) - y \right]^2 + [-L_b \cos \theta_1 - z]^2 = L_a^2 \\ \left[ -\frac{\sqrt{3}}{2} (R + L_b \sin \theta_2 - r) - x \right]^2 + \left[ \frac{1}{2} (R + L_b \sin \theta_2 - r) - y \right]^2 + [-L_b \cos \theta_2 - z]^2 = L_a^2 \\ x^2 + [-(R + L_b \sin \theta_3 - r) - y]^2 + [-L_b \cos \theta_3 - z]^2 = L_a^2 \end{cases} \quad (4)$$

The parameters of Delta mechanism are shown in Table 1.

Table 1

The parameters of Delta mechanism							
Symbol	$L_a/mm$	$L_b/mm$	$R/mm$	$r/mm$	$\eta_1$	$\eta_2$	$\eta_3$
Values	800	300	150	50	30°	150°	90°

There are three equations in the equation set (4). The forward kinematics analysis is carried out to obtain the workspace of the Delta mechanism. Taking the mobile platform center coordination  $(x, y, z)$  as the unknown quantities, the mobile platform center coordination can be resolved when the given value of each driving arm  $(\theta_1, \theta_2, \theta_3)$  is determined. Within the value range of  $\theta_i$ , the set of points of the Delta mechanism mobile platform can be obtained by the method of exhaustion (Liu et al., 2019; Zhang et al., 2019). The set of points can be densified in the three-dimensional coordinate system to get the Delta mechanism’s workspace.

**Numerical Simulation of Propane Combustion**

The burner, the key component of the flame weeding robot, is mainly composed of a base, a nozzle and a burner tip, whose diagram of real products is shown in Figure 4(a). When it is working, the propane is sprayed from the nozzle, which is mixed with air and burned in the burner. The burner tip diameter is determined to be 30 mm and its length is 75 mm according to the structure and the size of weeding robot, and its working environment.  $d$  represents the nozzle diameter and the two-dimensional model of burner is shown in Figure 4(b).

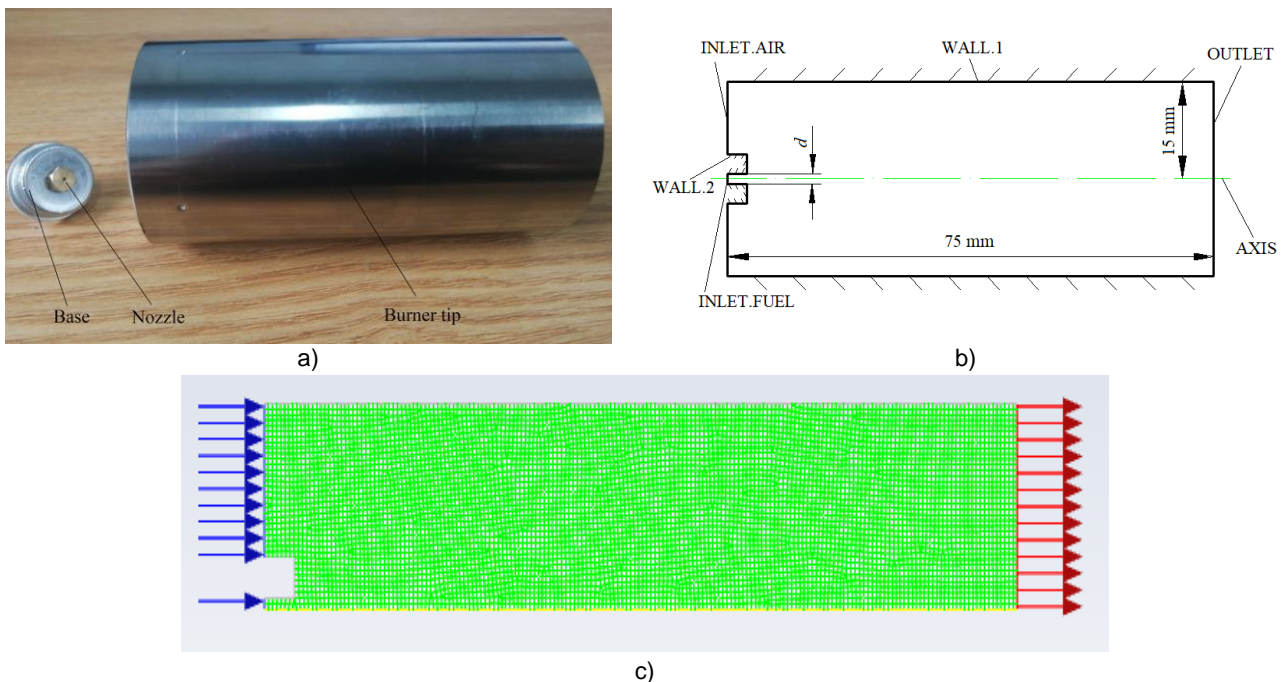


Fig. 4 - Burner model

The nozzle diameter directly affects the flame temperature distribution inside and out of the burner to further influence the effectiveness of weeding. There are a variety of nozzles with different diameters on the market.

To select the proper nozzle that is applicable to this weeder, the numerical simulation of propane combustion is carried out by Fluent on two burners whose diameters  $d$  are 0.8 mm and 1.6 mm, respectively. The main process is as follows. Firstly, the burner cross-section model is established by ANSYS ICEM CFD and is divided by the gridding, which is shown in Figure 4(c). Read the gridding and set up the solver parameters on the Fluent. Activate the option of Energy in the model settings (Tang et al., 2016). And then select the standard k-epsilon model for the turbulence model. In the dialogue box of the compositional model, activate the compositional transport and the option of the eddy-dissipation. Secondly, set up the boundary conditions and make sure that the fuel inlet velocity is set as 2.5 m/s and the air inlet velocity is set as 0.2 m/s. Lastly, the iterative computations is performed after the setting of iterative residual and the initialization of flow field.

## RESULTS

### Workspace Solutions and Analysis

The range of each field angle is determined to be  $5^\circ \leq \theta_i \leq 110^\circ$  by the structure size of the flame weeding robot. The method of exhaustion is performed to program and solve the equation, drafting the Delta mechanism workspace in the three-dimensional coordinate system, as shown in Figure 5.

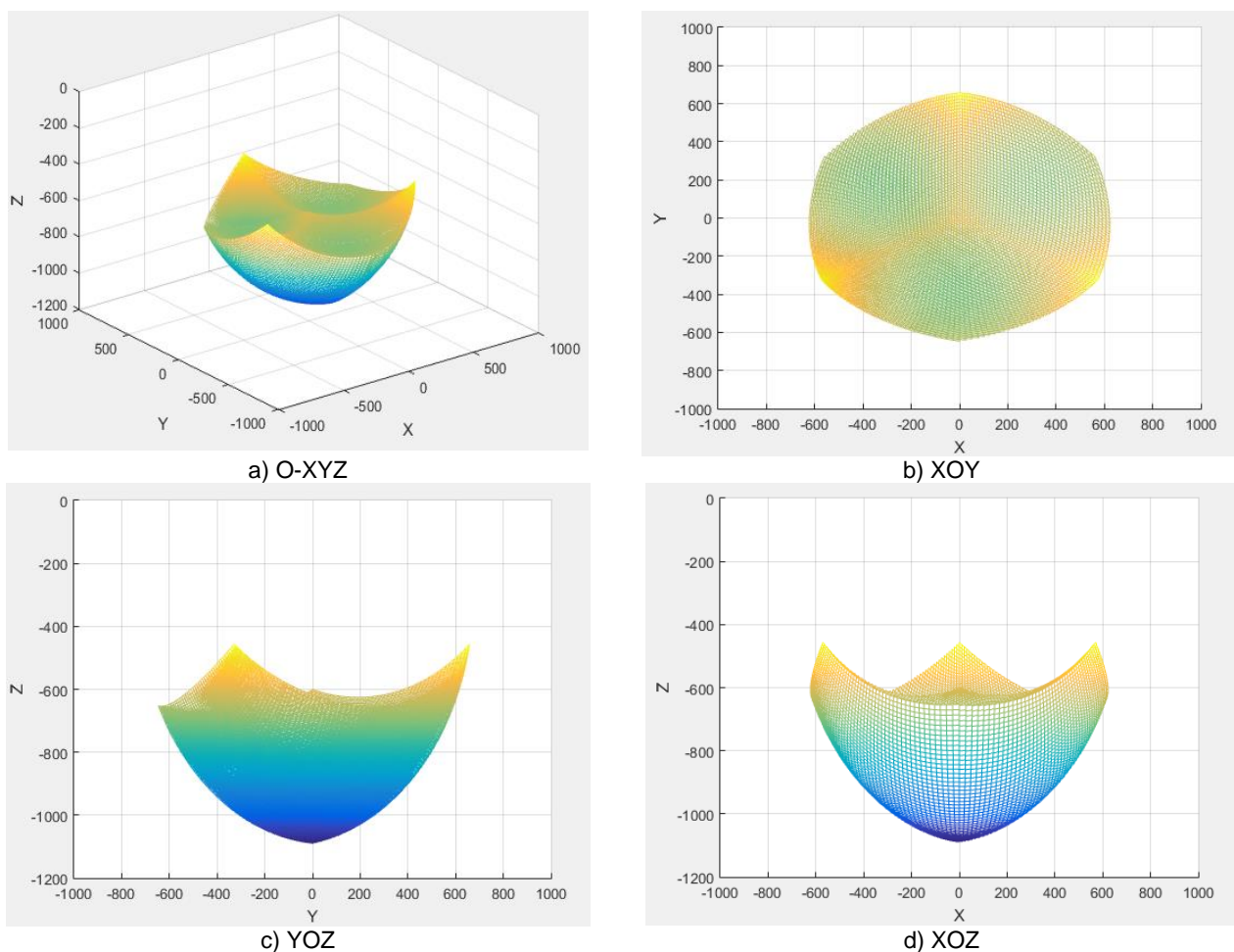


Fig. 5 - Workspace of Delta mechanism

The full-scale workspace of the Delta mechanism is the three-dimensional space in the enveloping surface, as shown in Figure 5 (a), and Figure 5 (b), (c) and (d) represent the projections of workspace on the planes of XOY, YOZ and XOZ, respectively. It can be seen from Figure 5(b) that the minimum value of x is -622.4 mm, the maximum value is 622.4 mm, the minimum value of y is -646.2 mm, and the maximum value is 658.2 mm. It can be known from Figure 5(c) and 5(d) that the minimum value of z is -1089 mm and the maximum value is -456.2 mm. The sectional view of XOZ plane is drawn by the full-scale workspace of the Delta mechanism, as shown in Figure 6. It can be seen from Figure 6 that the smart workspace can satisfy the formulas (1) and (2) simultaneously when its bottom surface diameter  $D$  is 400 mm and the height  $H_1$  is 359.8 mm.

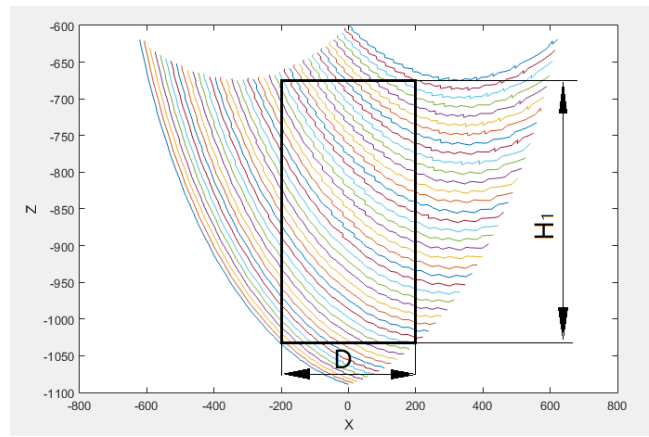


Fig. 6 –Workspace section

**Numerical Simulation Results and Analysis**

The flame temperature distribution diagrams of two combust with nozzle diameters of 0.8 mm and 1.6 mm are shown in Figure 7 (a) and (b) by the numerical simulation of the propane combustion process. It can be seen that the maximum flame temperature during the propane combustion is in or near the center of the burner, and the maximum temperature is 1,830 K.

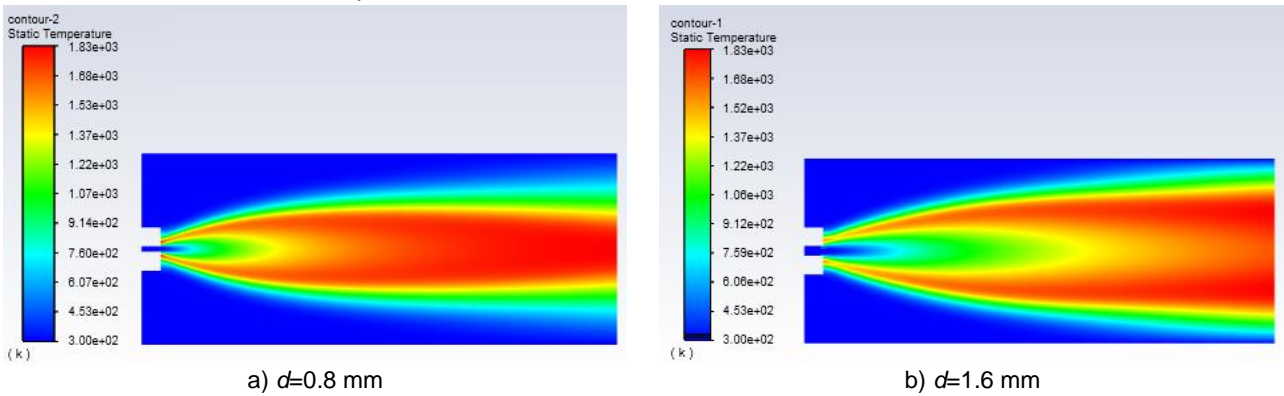


Fig. 7 - Temperature distribution inside burner

The CFD-Post module is utilized to have the post-process on the numerical simulation results to obtain the stereoscopic render effects of the flame temperature distributions in two burners, as shown in Figure 8 (a) and (b).

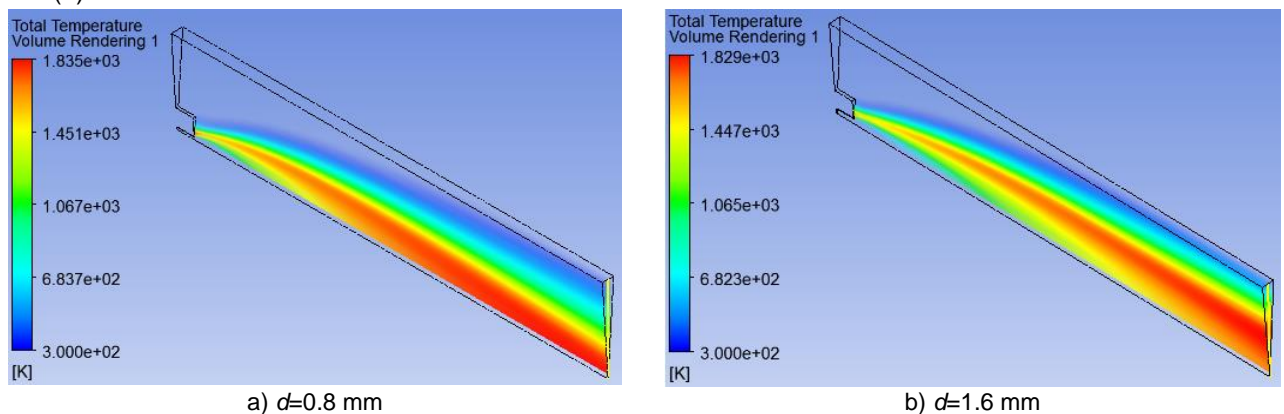


Fig. 8 -The stereoscopic render effects of the flame temperature distribution

To accurately obtain the burner outlet temperature distribution, it needs to take the center of the burner outlet as the starting point and draw a line segment that is perpendicular to the wall surface. Thus, the changing curve is displayed when each temperature on the output line segment changes with different positions. As shown in Figure 9 (a) and (b), the minimum scale value on the abscissa should be 0.5mm in accordance with the distance between the abscissa representative point and the center of the burner outlet, and the ordinate represents the temperature.

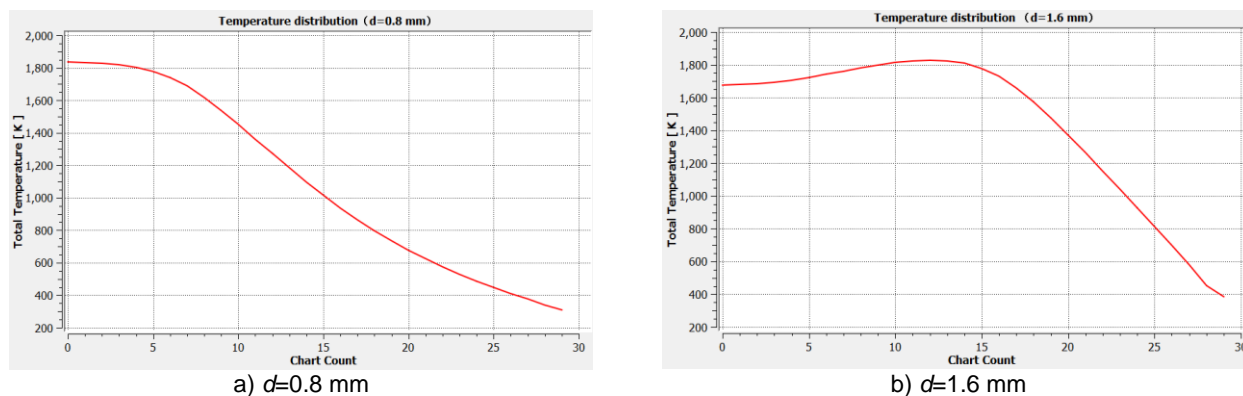


Fig. 9 - Burner outlet temperature variation curve

Comparing with Figure 9(a) and (b), it can be seen that the maximum flame temperatures are close at the outlets of two burners whose nozzle diameters are 0.8 mm and 1.6 mm, respectively. Owing to the symmetrical temperature distribution in the burner outlet, it can be deduced that the flame widths are 21.5 mm and 27 mm respectively when the temperatures at those two outlets are above 600 K, namely when the nozzle diameter is 1.6 mm, the burner outlet has a wider high temperature flame, which meets the requirements of the flame weeding.

## CONCLUSIONS

(1) Taking vegetable seedlings as research object, a flame intra-row weeding robot was designed in this paper based on the Delta mechanism. The analysis on the workspace of the Delta mechanism shows that the smart workspace meets the weeding requirements on the condition that the length of the driving arm is 300 mm, the length of the driven arm is 800 mm, the radius of the static platform is 150 mm, and the radius of the mobile platform is 50 mm.

(2) The numerically simulation on the propane combustion process in the burner was performed by the Fluent component transport model. When the nozzle diameter took different values, the analysis on the temperature distribution inside and out of the burner showed that it meets the flame weeding technical requirements on the condition that the nozzle diameter is 1.6 mm, the highest temperature is 1,830 K, and the width of the high temperature zone is 27 mm.

## ACKNOWLEDGEMENTS

This research, titled “Workspace Analysis of a Flame Intra-row Weeding Robot in Vegetable Field and Numerical Simulation of Propane Combustion”, was funded by the Science and Technology Innovation Fund of Shanxi Agricultural University (2017015), by project: “Major Special Projects for the Construction of China Modern Agricultural Industrial Technology System (Grant No. CARS-07-D-2)”.

## REFERENCES

- [1] Deng M.Y., (2018), Mineral Content and Nutritional Value Evaluation and Risk Assessment in Vegetables (蔬菜中矿物质含量测定、营养评价及风险评估). *Food Research and Development*, Vol.39, Issue 9, pp.97-102, Tianjin / P.R.C.;
- [2] Xiao T.Q., (2017), Development status of vegetable production and its mechanization in China (我国蔬菜生产概况及机械化发展现状). *Journal of Chinese Agricultural Mechanization*, Vol.38, Issue 8, pp.107-111, Nanjing / P.R.C.;
- [3] Chen Z.W., (2015), Study review and analysis of high performance intra -row weeding robot (智能高效株间锄草机器人研究进展与分析). *Transactions of the Chinese Society of Agricultural Engineering*, Vol.31, Issue 5, pp.1-8, Beijing / P.R.C.;
- [4] Liu W., (2017), Research Status of Mechanical Intra—Row Weed Control in Row Crops (作物株间机械除草技术的研究现状). *Journal of Agricultural Mechanization Research*, Vol.39, Issue 01, pp.243-250, Harbin / P.R.C.;
- [5] Wu T., (2019), Analysis and Study on Intelligentized Technologies of Intra-row Weeding Mechanical Control (智能化作物株间机械除草技术分析与研究). *Journal of Agricultural Mechanization Research*, Vol.41, Issue 6, pp. 7- 12+18, Harbin /P.R.C.;



- [6] Wang H.C., (2018), Study Status of the End-actuator of Intra-row Weeding Machine. *Journal of Anhui Agricultural Sciences*, Vol. 46, Issue 17, pp.22-26+29, Hefei / P.R.C.;
- [7] Hu L., (2012), Development and experiment of intra-row mechanical weeding device based on trochoid motion of claw tooth (基于爪齿余摆运动的株间机械除草装置研制与试验). *Transactions of The Chinese Society of Agricultural Machinery*, Vol.28, Issue 14, pp. 10- 16, Beijing / P.R.C.;
- [8] Huang X.L., (2012), Optimal Design of Rotating Disc for Intra-row Weeding Robot (苗间锄草机器人锄草刀优化设计). *Transactions of the Chinese Society for Agricultural Machinery*, Vol.43, Issue 6, pp.42-46, Beijing / P.R.C.;
- [9] Jiang Y., (2020), Design and experiment of pneumatic paddy intra-row weeding device (气动式水稻株间机械除草装置研制). *Journal of South China Agricultural University*, Vol.41, Issue 6, pp.37-49, Guangzhou / P.R.C.;
- [10] Zhou F.J., (2018), Design and Experiment of Cam Rocker Swing Intra-row Weeding Device for Maize (凸轮摇杆式摆动型玉米株间除草装置设计与试验). *Transactions of the Chinese Society for Agricultural Machinery*, Vol.49, Issue 1, pp.84-92, Beijing / P.R.C.;
- [11] Han B., (2020), Design and Experiment of Soybean Intra-row Weeding Monomer Mechanism and Key Components (大豆株间除草单体机构及关键部件设计与试验). *Transactions of the Chinese Society for Agricultural Machinery*, Vol.51, Issue 06, pp.112-121, Beijing / P.R.C.;
- [12] Reiser D., (2019), Development of an Autonomous Electric Robot Implement for Intra-Row Weeding in Vineyards. *Agriculture*, Vol.9, Issue 1, pp. 18-29, Basel / Switzerland;
- [13] Kumar S.P., (2020), A fuzzy logic algorithm derived mechatronic concept prototype for crop damage avoidance during eco-friendly eradication of intra-row weeds. *Artificial Intelligence in Agriculture*, Vol.4, pp.116-126, Amsterdam / Netherlands;
- [14] Wang J.W., (2021), Design and Experiment of Jet-type Paddy Field Weeding Device between Plants (射流式水田株间除草装置设计与试验). *Transactions of the Chinese Society for Agricultural Machinery*, <http://kns.cnki.net/kcms/detail/11.1964.S.20210917.1058.004.html>. Beijing / P.R.C.;
- [15] Rajković M., (2021), Sustainable Organic Corn Production with the Use of Flame Weeding as the Most Sustainable Economical Solution. *Sustainability*, Vol.13, Issue 2, pp. 572-583, Basel / Switzerland;
- [16] Raja R., (2020a), Real-time weed-crop classification and localization technique for robotic weed control in lettuce. *Biosystems Engineering*, Vol.192, Issue 4, pp. 257-274, Amsterdam / Netherlands;
- [17] Trygve U., (2018), Robotic in-row weed control in vegetables. *Computers and Electronics in Agriculture*, Vol.154, Issue 11, pp. 36-45, Amsterdam/Netherlands;
- [18] Raja R., (2020b), Real-time robotic weed knife control system for tomato and lettuce based on geometric appearance of plant labels - ScienceDirect. *Biosystems Engineering*, Vol.194, Issue 6, pp. 152-164, Amsterdam / Netherlands;
- [19] Kennedy H., (2020), Crop signal markers facilitate crop detection and weed removal from lettuce and tomato by an intelligent cultivator. *Weed Technology*, Vol.34, Issue 3, pp. 342-350, Lawrence / USA;
- [20] Knezevic S. Z., (2014), Growth stage affects response of selected weed species to flaming. *Weed Technology*, Vol.28, Issue 1, pp. 233-242, Lawrence / USA;
- [21] Guan P., (2019), Research and realization of key Technology of Flame weeding Machine for Chinese Medicinal Materials (中药材火焰除草机关键技术研究及实现). Master Degree Dissertation, Shanxi Agricultural University, Taiyuan / P.R.C.;
- [22] Fu X.M., (2016), Review on Weed Management in Organic Orchards at Home and Abroad (国内外有机果园杂草管理技术研究综述). *Weed Science*, Vol.34, Issue 04, pp.7-11, Beijing / P.R.C.;
- [23] Zhang M.W., (2018), *Principle and application of industrial robot: DELTA parallel robot* (工业机器人原理及应用: DELTA 并联机器人), ISBN 9787560373171, Harbin University of Technology Press, P.R.C.
- [24] Liu L., (2019), Workspace simulation and trajectory planning for tomato sorting Delta robot, *INMATEH-Agricultural Engineering*, Vol. 58, Issue 2, pp.177-186, Bucharest / Romania.
- [25] Zhang X.C., (2019), Trajectory Planning for Product Sorting and Error Analysis of a Delta Parallel Robot (Delta 机器人产品分拣轨迹规划仿真). *Computer Simulation*, Vol.36, Issue 11, pp.295-299+364, Guangzhou / P.R.C.;
- [26] Tang J.P., (2016), *ANSYS fluent 16.0 super learning manual* (ANSYS FLUENT 16.0 超级学习手册), ISBN 9787115422040, Posts and Telecommunications Press, Beijing / P.R.C.